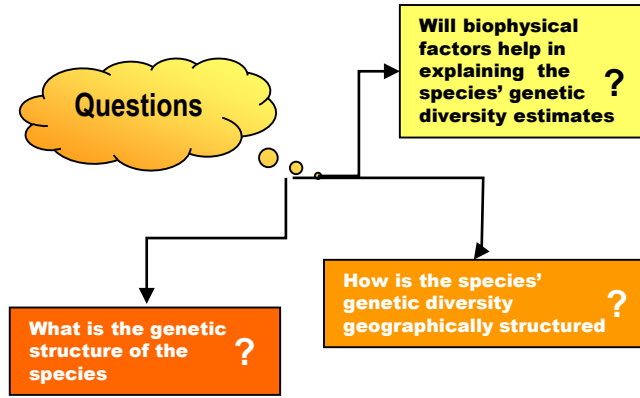


Application of biophysical factors and molecular markers to explain spatial genetic structure in strawberry tree using GIS tools

Ribeiro, M.M.^{1,2*}, Quinta-Nova L.^{1,3}, Roque N.¹, Ricardo A.^{1,4}, Gaspar D.⁴, Costa R.^{2,4}, Vendramin G.G.⁵

¹ Polytechnic Institute of Castelo Branco, School of Agriculture, Dep. Natural Resources and Sustainable Development, 6001-909 Castelo Branco, Portugal. Email: mataide@ipcb.pt ²Forest Research Center, School of Agriculture, University of Lisbon, Portugal. ³Research Center for Natural Resources, Environment and Society, Castelo Branco, Portugal. ⁴ Instituto Nacional de Investigação Agrária e Veterinária, Laboratório de Biologia Molecular, Av. da República, Quinta do Marquês, 2784-159, Oeiras, Portugal. ⁵ Institute of Biosciences and BioResources, National Research Council, Via Madonna del Piano 10, 50019 Sesto Fiorentino (Firenze), Italy.

PURPOSE OF THE STUDY



RESULTS

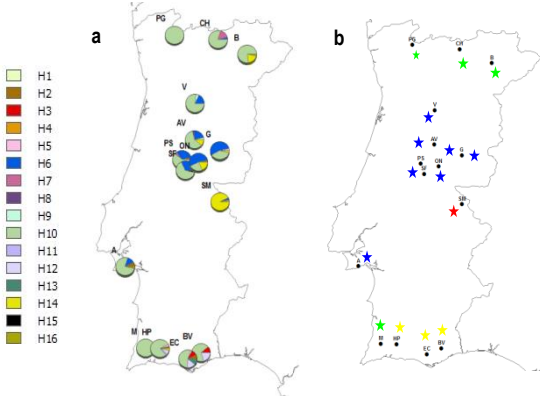


Fig 3. Distribution of 16 haplotypes in populations. The numbers indicate the code of the haplotype (a). Populations clustering with cpSSR data and stands coordinates using BAPS, a Bayesian approach (b).

MATERIAL AND METHODS

- 15 natural populations and 30 ind./pop.
- 4 maternally inherited cpSSRs
- Genetic differentiation among populations estimated by R_{ST} and G_{ST}
- Populations clustering using a Bayesian approach and stand coordinates: BAPS
- Biophysical and genetic diversity data were analyzed using XLSTAT to built the PCA

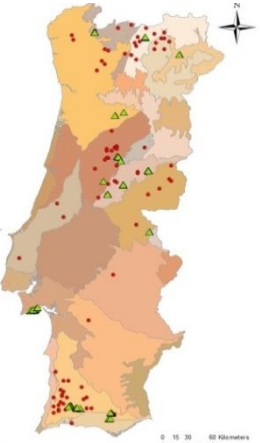


Fig. 1. Natural populations (green triangles) and natural stands recorded in the Forest Inventory 2006 (red dots).

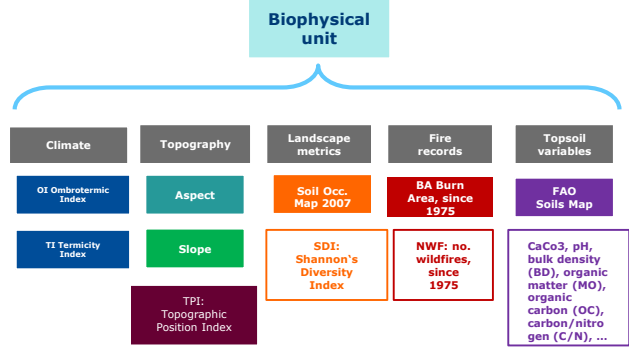


Fig. 2 Biophysical variables were studied using GIS (Geographic Information Systems) in the biophysical unit = the area spanning 1 km from each one of the 30 stand trees.

TAKE HOME

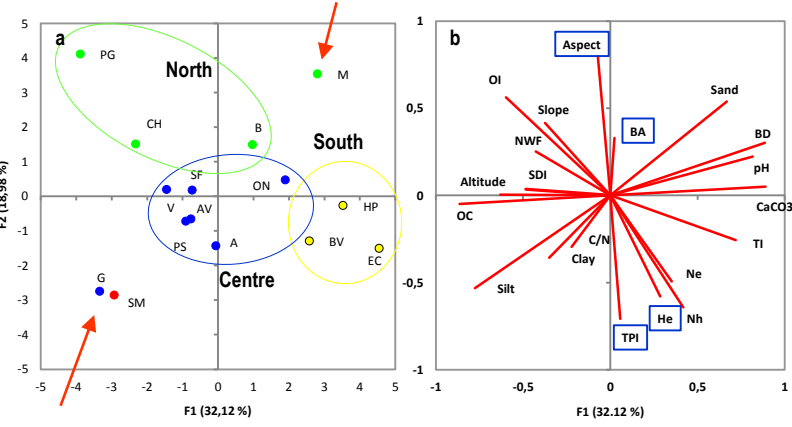


Fig 4. Principal component analysis (PCA) performed with the biophysical factors, see Fig. 2 for label details, and genetic diversity estimates (He = haplotypic diversity, Nh = no. of haplotypes, Ne = effective no. of haplotypes). The observations (populations) (a) and the variables (b). Red arrows point at putative outliers. The total of the variance explained with $F1$ and $F2$ is 51,1%.

Acknowledgements: This work was supported by the grant from FCT PTDC/AGR-FOR/3746/2012 (Arbutus unedo plants and products quality improvement for the agro-forestry sector). Thanks to Ilaria Spanu assistance in the laboratorial analysis, also extended to Dragos Postolache that also helped us to produce the haplotypic map. Thanks are extended to Francesca Bagnoli that kindly introduced us in the data analysis with the Bayesian approach.

A high among population differentiation was observed ($G_{ST}=28.8\%$) and even a stronger R_{ST} (54.8%) value was found, indicating a strong geographical structure, due, probably, to low gene flow through pollen.

A clear clustering in 3 groups was untangled by the Bayesian analysis (Fig 3b) and also supported both by the distribution of the haplotypes (Fig. 3a) and the PCA observations' projection (Fig. 4a): the Northern, the Central and the Southern populations

One outlier is clear in Fig 3b with a red star: the SM population, with an haplotypic pattern clearly different from all the others (Fig 3a), and a low He value (13%). Two other populations have probably experienced a bottleneck effect due to the impact of wildfires: PG and M. Indeed they have $He=0$ and only one haplotype.

The genetic diversity estimates (He, Nh and Ne) are inversely correlated to the burn area (BA) and the Aspect, though the former is only partially explained by the 2nd factor (Fig 4b), and directly correlated with the TPI (a rugosity index). Future work will include the use of nuclear microsatellites to improve the power to identify the factors that are responsible for the observed spatial structuring of species' genetic diversity.